Modeling and Optimization of Wireless Channel in High-Speed Railway Terrain

JIANLI XIE, CUIRAN LI, (Member, IEEE), WENBO ZHANG, AND LING LIU

School of Electronic and Information Engineering, Lanzhou Jiaotong University, Lanzhou 730070, China

Corresponding author: Cuiran Li (licr@mail.lzjtu.cn)

ABSTRACT The high-speed railway (HSR) wireless channel models based on field measurements have poor universality and low modeling accuracy due to the limitations of the experimental methods and the terrain conditions. To overcome this problem, this paper considers the wireless channels in various HSR scenarios (such as tunnels, mountains, viaducts, cuttings and plains) as the research objects and establishes a novel finite-state Markov chain (FSMC) optimization simulation model based on the signal-to-noise ratio (SNR) threshold, the channel states and the state transition probability matrix, by using the nonuniform space division SNR quantization strategy (hereinafter referred to as Strategy 1) and the equal-area space division SNR quantization strategy (hereinafter referred to as Strategy 2). The SNR curves that are obtained via simulation closely fit the experimental results; therefore, the proposed simulation model can accurately characterize the channel state in a variety of HSR scenarios. Furthermore, the simulation results demonstrate that in the tunnel scenario, Strategy 1 realizes a smaller mean square error (MSE) and a higher modeling accuracy than Strategy 2. The MSE values of the two strategies are similar in the plain scenario. Strategy 2 realizes a smaller MSE and a higher modeling accuracy in the mountain, viaduct and cutting scenarios.

INDEX TERMS Channel models, high-speed railway, Markov processes, railway communication, SNR quantization strategy.

I. INTRODUCTION

With the fast deployment of high-speed railway (HSR) systems in the past several years, the speed of HSR has been increasing and typically reaches 200 km/h-350 km/h [1], [2]. In addition to the high mobility of the train, there are growing demands on high-speed data services. To meet these demands, HSR wireless communication systems must overcome many problems, such as complex and changeable HSR scenarios [3], [4], fast handoff [5] and Doppler shift [6], among others. Therefore, the accurate recognition of HSR wireless channels will facilitate the development, performance optimization and parameter setting of HSR communication systems.

High-speed trains travel through a variety of scenarios resulting in the diversity of wireless channels. According to the channel fading characteristics of HSR scenarios, different modeling methods are used to model the wireless channel,

The associate editor coordinating the review of this manuscript and approving it for publication was Ke Guan.

such as deterministic modeling, semi-deterministic modeling and statistical modeling. Different channel models are established according to different modeling methods. In [7]–[9], a deterministic channel model of ray tracing algorithm is proposed, which is commonly used in tunnels, viaducts and other environments. In [10], [11], the geometric random model is used, which is a semi-deterministic modeling method. This modeling method has a good fit with the actual environment and the complexity is not high. The [12], [13] use statistical modeling method, in which [12] analyzes the angle characteristics and the spatial correlation of HSR channels based on a new measurement scheme of the mobile virtual antenna array (MVAA). In addition, the angle power spectrum and angle expansion are studied, and the measurement results are modeled statistically. In [13], a tap delay model (TDL) is proposed based on the analysis of the characteristics of delay spread and Doppler frequency shift spread in HSR hills.

In this paper, we study finite-state Markov chain (FSMC) channel modeling in various typical HSR scenarios, and establish an FSMC model between the base station (eNB) and

the relay on the top of the train. The main contributions are as follows:

- Based on the path-loss model in each HSR scenario, the equal-area space division strategy and the nonuniform space division strategy are used to divide the relative position of the high-speed train and the eNB, so as to improve the accuracy of the channel model.
- Based on the comparison of MSE, the accuracy of two FSMC channel modeling strategies in different HSR scenarios is analyzed, and compared with the uniform space division method, so as to realize the FSMC channel modeling suitable for different HSR scenarios.

The remainder of the paper is organized as follows: Section II describes the related work of the FSMC model. Section III describes the FSMC model. Section IV divides the distance between the eNB and the relay into nonuniform spaces and equal-area spaces, and determines the SNR threshold and the channel state values according to the path-loss model of each scenario. The simulation results are presented in Section V, which compares and analyzes FSMC models that are constructed via Strategy 1 and Strategy 2 in terms of MSE. Finally, the conclusions of this study are presented and discussed in Section VI.

II. RELATED WORKS

In wireless fading channel modeling, the FSMC model is adopted by many scholars. In [14], the nonstationary characteristic is studied by using Markov chains to describe the wireless signal propagation mechanism in the HSR viaduct scenario. Based on the channel measurements of Beijing-Tianjin HSR, the transition probability matrix and the steady-state probability matrix of the Markov chains are determined, and the similarities between the simulation results of models of various orders and the measured data are analyzed in terms of the Kullback-Leibler distance. In [15], an FSMC channel model is established for HSR fading channels, which considers the influence of speed on the model, and an expression of the state transition probability is derived. In addition, a new FSMC channel model is proposed in [16], which takes into account the fast fading characteristics in high-speed environment. The exact expression of the state transition probability between any two channel states is obtained, and the accuracy of the model is evaluated.

In [17], a new modeling method is proposed, which uses the state transition probability of economics in FSMC modeling, and the received average SNR is divided equally by using the substitution probability. Compared with the other FSMC modeling, the modeling method in [17] has less computational complexity. An FSMC model based on the WINNER II channel for HSR scenarios is proposed in [18], and the validity of the model is demonstrated. However, the model lacks the measured data. In [19], the channel modeling between wireless sensors and high-speed trains in a viaduct scenario is studied. The communication distance between the high-speed train and the ground sink node is nonuniformly divided

TABLE 1. Notations.

γ_k	The channel state in time slot k
N	The number of SNR levels
Γ_n	The threshold of the nth level of SNR
$p_{i,j}^l$	The transition probability from state S_i to state S_j in the lth sub-space
S_i^l	The channel state i in the lth sub-space
$\boldsymbol{P}^l$	The transition probability matrix in the lth sub-space
D	The distance between the transmitter and the receiver
M	The number of spaces
T	The number of sub-spaces

into several intervals according to the free-space path-loss model, and an FSMC model is established in each interval. This paper ideally use a free-space path-loss model to predict the path-loss values at the receiver in the viaduct scenario.

In practical HSR scenarios, there exist many scatterers, and the signal will be subjected to a variety of signal propagation mechanisms, which will substantially affect the received SNR. Therefore, the free-space path-loss model is not suitable for practical HSR scenarios. In this paper, the path-loss values take the measured data in the literature [21]–[24] as references for FSMC channel modeling in various HSR scenarios. In the above literatures, the multi-antenna wireless broadband channel detector (Proposound) of Finland's Elite Bit was selected when measuring the viaduct and cutting. In the test process, the receiving antenna uses the dedicated roof-top HUBER + SUHNER to receive the excitation signal, which avoids the penetration loss of the windows and compartments. Both the transmitter and receiver use an external global positioning system GPS clock as the frequency reference. In addition, the real-time train speed and location information is also acquired through GPS equipment.

III. FSMC CHANNEL MODEL IN HSR SCENARIOS

The FSMC model is a statistical model that has been widely used in fading channel modeling. The main strategy of FSMC is to characterize the channel states with finite discrete values and map them into Markov states.

In this paper, the FSMC model is constructed via the method that is proposed in [17], and the channel state is represented by the average SNR. In each HSR scenario, the average SNR of the receiver changes nonlinearly with the distance between the transmitter and the receiver due to the high mobility of the train. Therefore, the communication distance between the eNB and the relay is divided into n nonuniform and nonoverlapping spaces, and each space is divided into several uniform sub-spaces. Then, FSMC is used to track the channel state in each sub-space.

In the lth sub-space, let $\Gamma = (\Gamma_0, \Gamma_1, \ldots, \Gamma_{N-1})$ be the SNR threshold vector of N elements, where $\Gamma_0 < \Gamma_1 <$

$\ldots < \Gamma_{N-1}$ and Γ_0 and Γ_{N-1} are the maximum and the minimum values of SNR in this sub-space. Assuming that the train passes through each sub-space at a constant speed and the total time of the train passing through the sub-space is discretized into several equal time slots, to represent the duration of the communication between the eNB and the relay in each space, let γ_k denote the SNR of the received signal in time slot k. If $\gamma_k \in [\Gamma_{n-1}, \Gamma_n]$, then the channel state is S_i in time slot k, namely, $\gamma_k = S_i$[20]. The channel state transition probability is expressed as

$$p_{i,j}^l = P\left\{\gamma_{k+1} = S_j \,|\, \gamma_k = S_i\right\} \tag{1}$$

where $k = 1, 2, \ldots, n$, $i, j \in \{0, 1, 2, \ldots, N-1\}$, and the probability of being in state S_i is defined as

$$p_i^l = p\{\gamma_k = S_i\} \tag{2}$$

In this paper, only the first-order Markov model is considered, namely, it is assumed that the state transition only occurs between the current state and an adjacent state

$$p_{i,j}^l = 0, \quad \text{if } |j - i| > 1 \tag{3}$$

The transition probability in lth sub-space is represented by a probability matrix of size $N \times N$, where each row of elements satisfies the following requirements.

$$\sum_{j=0}^{N-1} p_{i,j}^l = 1, \quad i \in \{0, 1, \ldots, N-1\} \tag{4}$$

IV. FSMC WIRELESS CHANNEL MODELLING
In this section, the corresponding average SNR is obtained based on the path-loss models of various HSR scenarios. Then, the communication distance between the transmitter and the receiver is divided according to two strategies, namely, nonuniform space division and equal-area space division, and FSMC channel modeling is conducted.

A. PATH LOSS FOR VARIOUS HSR TERRAINS
The signal will be affected by buildings, trees and undulating terrain during the signal propagation. The received signal will change dramatically, thereby resulting in the phenomenon of fading. In this paper, the path-loss values take the measured data in the literature [21]–[24] as references for FSMC channel modeling in various HSR scenarios. Some of the path-loss models take the shadow fading into account, while the others do not. In order to facilitate the analysis of the modeling experimental results of each scenario, we have made a unified treatment, that is, the shadow fading is not considered, so as not to affect the SNR quantization strategy.

According to [21]–[24], the signal fading differs among HSR scenarios, and the path-loss models in various scenarios
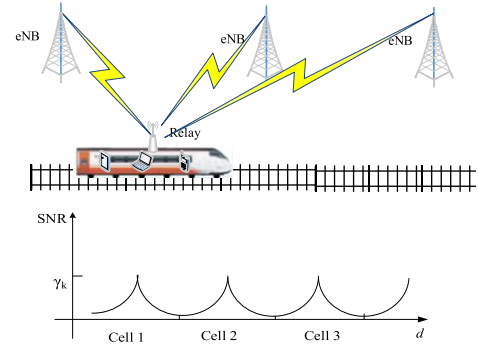

FIGURE 1. Variation of SNR with T-R distance.

are as follows.

$$PL(d) = \begin{cases} 34.45 + 18.69 \log(d + d_0) & \text{(tunnel)} \\ \begin{aligned} &32.4 + 23.11 \\ &\quad \log(d + d_0), \quad d < 500m \\ &-9.15 + 38.11 \\ &\quad \log(d + d_0), \quad d \geq 500m \end{aligned} & \text{(mountain)} \\ 11.0 + 42.4 \log(d + d_0) & \text{(viaduct)} \\ 17.5 + 36.1 \log(d + d_0) & \text{(cutting)} \\ 20.9 + 25.3 \log(d + d_0) & \text{(plain)} \end{cases} \tag{5}$$

where d represents the distance between the eNB and the relay, and d_0 is the reference distance. The average SNR at the receiver can be expressed as

$$\bar{\gamma}(d) = P_t - PL(d) - N_0 \tag{6}$$

where P_t is the transmission power and N_0 is the noise power. During the train operation, the received signal will change nonlinearly with the distance. When the train is near the eNB, the electromagnetic wave fluctuates substantially; when it is far away, its fluctuation is slower. Figure 1 depicts the periodic change of SNR at the receiver with distance in HSR. The interference of noise with the signal becomes large as the distance increases. Therefore, the communication distance of 500 m between the eNB and the relay is selected for investigation in this paper.

B. TWO WIRELESS CHANNEL MODELLING STRATEGIES
From (5) and (6), the SNR at the receiver in various HSR scenarios can be obtained.

$$\bar{\gamma}(d) = \begin{cases} P_t - 34.45 - 18.69 \log(d + d_0) - N_0 & \text{(tunnel)} \\ P_t - 32.4 - 23.11 \log(d + d_0) - N_0 & \text{(mountain)} \\ P_t - 11.0 - 42.4 \log(d + d_0) - N_0 & \text{(viaduct)} \\ P_t - 17.5 - 36.1 \log(d + d_0) - N_0 & \text{(cutting)} \\ P_t - 20.9 - 25.3 \log(d + d_0) - N_0 & \text{(plain)} \end{cases} \tag{7}$$
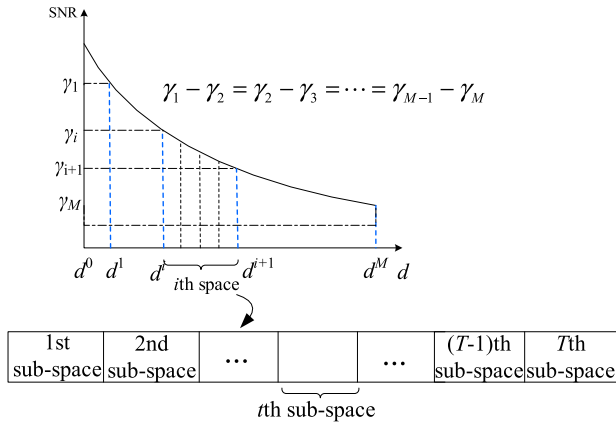
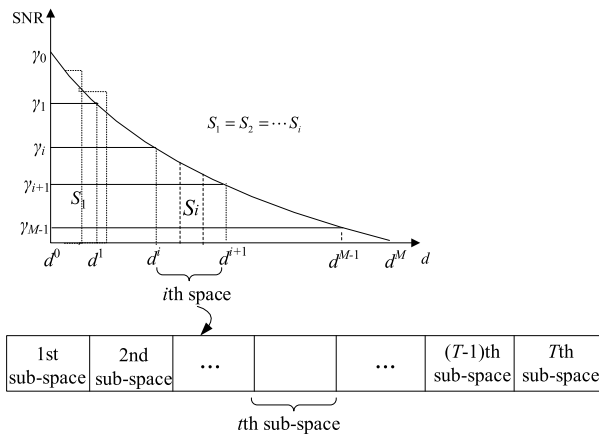**FIGURE 2.** The diagram of Non-uniform space division.

FIGURE 3. The diagram of equal area space division.

1) NON-UNIFORM SPACE DIVISION

The communication distance D between the eNB and the relay is divided into M non-uniform spaces, and the SNR values in each space are equal, namely, $\gamma_1 - \gamma_2 = \gamma_2 - \gamma_3 = \cdots = \gamma_{M-1} - \gamma_M$, Then, these spaces are divided into several sub-spaces equally, shown in Figure 2.

As can be seen from Figure 2,

$$\gamma_i = P_t - PL(0) - N_0 - i\frac{PL(D) - PL(0)}{Q} \quad (8)$$

According to (7) and (8), the reference distance of the each dividing points in a space can be obtained, namely, $d^0, d^1, \cdots, d^M$, where $d^0 = 0, d^M = D$. Then, the space (d^i, d^{i+1}) is evenly divided into T sub-spaces, where the sub-space length is $(d^{i+1} - d^i)/T$. Let $d_t^i, t = 0, 1, \ldots, T-1$, represents the tth division point in the sub-space.

$$d_t^i = d^i + t\frac{d^{i+1} - d^i}{T} \quad (9)$$

To facilitate calculation, d^i and d_t^i are regarded as integers in the simulation. The modeling process steps are as follows.

Strategy 1 FSMC Channel Modeling via Strategy 1

Input: the transmit power P_t; the noise power N_0; the communication distance D

Output: MSE

Step1: Space division based on path loss
1 calculate the average SNR $\bar{\gamma}(d) = P_t - PL(d) - N_0$
2 for $i = 0$ to M do
3 calculate $\gamma_i = P_t - PL(0) - N_0 - i\frac{PL(D) - PL(0)}{M}$
4 calculate the space dividing point d^i by $\bar{\gamma}(d)$ and γ_i
5 for $t = 0$ to $T - 1$ do
6 calculate the sub-space dividing point $d_t^i = d^i + t\frac{d^{i+1} - d^i}{T}$

Step2: Determine the SNR threshold, channel state value and state transition probability matrix

1 determine the probability distribution function of SNR in various HSR scenarios
2 calculate the steady-state probability of each state
$\pi_n = \int_{\Gamma_{n-1}}^{\Gamma_n} p(\gamma)d\gamma$
3 equal probability method needs to be satisfied $\pi_1 = \pi_2 = \cdots = \pi_N = (1/N)$
4 calculate the average SNR in each state $\bar{\gamma}_n = \frac{1}{\pi_n}\int_{\Gamma_{n-1}}^{\Gamma_n} \gamma p(\gamma)d\gamma$
5 calculate the state transition probability

$$p_{nj} = P\left\{\gamma_{k+1} = s_j \mid \gamma_k = s_n\right\} = \frac{p\left\{\gamma_{k+1} = s_j, \gamma_k = s_n\right\}}{p\left\{\gamma_k = s_n\right\}}$$

Step3: MSE analysis
Output MSE

---

2) EQUAL AREA SPACE DIVISION

The area that is enclosed by the average SNR function at the relay, X-axis and Y-axis is divided into M equal-area and nonoverlapping spaces. Then, each space is equally divided into several sub-spaces, as illustrated in Figure 3. The equation that is used to divide the area is as follows, where S is the total area of all spaces and S_i is the area of the ith space.

$$S = \int_0^D \gamma(x) - \gamma(D)dx \quad (10)$$

To distinguish the distance from d in the integral equation, the distance d is denoted by x, and D is the maximum distance between the relay and the eNB. The area that is enclosed by the SNR, X-axis and Y-axis is obtained on the graph, and each area is divided into T small areas evenly according to the following equation.

$$S_i = i\frac{\int_0^D \gamma(x) - \gamma(D)dx}{M} \quad (11)$$

$$d_t^i = d^i + t\frac{d^{i+1} - d^i}{T} \quad (12)$$

From (11) and (12), the distance value at the dividing point of the space can be obtained, namely, $d^0, d^1, \cdots, d^M$, where $d^0 = 0$ and $d^M = D$. Then, the space (d^i, d^{i+1}) is evenly divided into T sub-spaces, and the sub-space length is $(d^{i+1} - d^i)/T$. Let $d_t^i, t = 0, 1, \ldots, T-1$, represent the tth

division point in the sub-space. The modeling process steps are as follows

---

Strategy 2 FSMC Channel Modeling via the Strategy 2

Input: the transmit power P_t; the noise power N_0; the communication distance D

Output: MSE

Step1: Space division based on path loss

1 calculate the average SNR $\bar{\gamma}(d) = P_t - PL(d) - N_0$

2 area integration $S = \int_0^D \gamma(x) - \gamma(D)dx$

3 calculate $S_i = i \frac{\int_0^D \gamma(x) - \gamma(D)dx}{M}$

4 calculate the space dividing point d^i by $\bar{\gamma}(d)$ and S_i

5 for $t = 0$ to $T - 1$ do

6 calculate the sub-space dividing point $d_t^i = d^i + t\frac{d^{i+1} - d^i}{T}$

   Step2: Determine SNR threshold, channel state value and state transition probability matrix

1 determine the probability distribution function of SNR in different HSR scenarios

2 calculate the steady-state probability of each state $\pi_n = \int_{\Gamma_{n-1}}^{\Gamma_n} p(\gamma)d\gamma$

3 equal probability method needs to be satisfied $\pi_1 = \pi_2 = \cdots = \pi_N = (1/N)$

4 calculate the average SNR in each state $\bar{\gamma}_n = \frac{1}{\pi_n}\int_{\Gamma_{n-1}}^{\Gamma_n} \gamma p(\gamma)d\gamma$

5 calculate the state transition probability

$$p_{nj} = P\left\{\gamma_{k+1} = s_j \,|\, \gamma_k = s_n\right\} = \frac{p\left\{\gamma_{k+1} = s_j, \gamma_k = s_n\right\}}{p\left\{\gamma_k = s_n\right\}}$$

   Step3: MSE analysis
   Output MSE

C. DETERMINATION OF THE SNR PROBABILITY DISTRIBUTION AND THE SNR THRESHOLD

It is highly important to determine the distribution of SNR during the division of the SNR threshold. Classical models are available for describing the fading distribution, such as the Rician [25], [26], Rayleigh [27], [28] and Nakagami-m [29] distributions. Due to the characteristics of the tunnel scenario, the Nakagami-m distribution, which is used in this paper, can more closely match the real data in tunnels while being consistent with the fading distribution of SNR at the receiver. Its distribution [30] is

$$p(\gamma^l) = \frac{(\mu^l)^{\mu^l}(\gamma^l)^{\mu^l - 1}}{(\bar{\gamma}^l)^{\mu^l}\Gamma(\mu^l)}\exp\left(-\frac{\mu^l\gamma^l}{\bar{\gamma}^l}\right) \qquad (13)$$

where γ^l is the SNR in the lth sub-space, $\bar{\gamma}^l$ is the mean value of the SNR in the lth sub-space, μ^l is the Nakagami fading factor in the lth sub-space, and $\Gamma(\cdot)$ is the gamma function. In the simulation, μ^l can be obtained via maximum likelihood estimation for each sub-space.

Due to the presence of scatterers in other HSR scenarios, such as trees and buildings, not only line of sight (LOS) paths but also nonline of sight (NLOS) paths are followed during

the signal propagation. Therefore, the Rician channel model can be used to approximate the SNR fading distribution. The equation [18] is as follows:

$$p(\gamma^l) = \frac{K^l + 1}{\bar{\gamma}^l}\exp\left[-K^l - \frac{(K^l + 1)\gamma^l}{\bar{\gamma}^l}\right]$$
$$\cdot I_0\left[\sqrt{\frac{4K^l(K^l + 1)\gamma^l}{\bar{\gamma}^l}}\right] \qquad (14)$$

where K^l is the fading factor in the lth sub-space, $I_0[\cdot]$ is the zero-order modified Bessel function of the first kind, $\bar{\gamma}^l$ is the average SNR. Both the K^l and $\bar{\gamma}^l$ can be estimated via the maximum likelihood function.

After obtaining the probability distribution function of SNR in each HSR scenario, the SNR threshold and each state value should be determined, which are especially important for FSMC channel modeling. To select the SNR threshold, the equal probability method [31], the Lloyd-Max method [32] and other methods can be used. In practice, a suitable method must be selected according to the application requirements. The equal probability method has been widely used in studies on Markov models for wireless fading channels. In this paper, the equal probability method is used to determine the SNR threshold.

The steady-state probability of each state can be obtained from the probability distribution function of SNR as

$$\pi_n = \int_{\Gamma_n}^{\Gamma_{n+1}} p(\gamma)d\gamma, \quad n = 1, 2, \ldots, N \qquad (15)$$

According to the equal probability method, $\pi_1 = \pi_2 = \cdots = \pi_N = (1/N)$, and the SNR thresholds are determined by the following requirement

$$\pi_n = \int_{\Gamma_n}^{\Gamma_{n+1}} p(\gamma)d\gamma = \frac{1}{N} \qquad (16)$$

The average SNR in each state can be expressed as

$$\bar{\gamma}_n = \frac{1}{\pi_n}\int_{\Gamma_n}^{\Gamma_{n+1}} \gamma p(\gamma)d\gamma, \quad n = 1, 2, \ldots, N \qquad (17)$$

After dividing the SNR thresholds of each state, the average SNR of the state can be obtained and expressed as the channel state. Then, the first-order state transition probability of the FSMC model is determined according to the conditional probability.

$$p_{n,j} = P\left\{\gamma_{k+1} = s_j \,|\, \gamma_k = s_n\right\} = \frac{p\left\{\gamma_{k+1} = s_j, \gamma_k = s_n\right\}}{p\left\{\gamma_k = s_n\right\}} \qquad (18)$$

V. SIMULATION EXPERIMENTS AND ANALYSIS

In this section, FSMC wireless channel models are established for various HSR scenarios via Strategy 1 and the Strategy 2. The simulation parameters are presented in Table 2.

TABLE 2. Simulation parameters.

	P_t/dBm	N_0/dBm
tunnel	0	-105
mountain	47	-49.7
viaduct	45	-85
cutting	45	-70
plain	47	-59.6

TABLE 3. SNR thresholds in the space [150 230] (arched tunnel).

	[150 158]	[158 166]	[166 174]	[174 182]	[182 190]
1st	25.50	29.50	26.00	30.00	26.50
2nd	27.12	31.47	28.74	31.25	28.51
3rd	28.75	33.33	31.19	32.50	30.36
4th	30.37	35.19	33.64	33.75	32.22
5th	32.00	37.00	36.00	35.00	34.00
	[190 198]	[198 206]	[206 214]	[214 222]	[222 230]
1st	27.00	18.00	19.00	26.00	28.00
2nd	27.75	21.93	21.50	29.90	30.69
3rd	28.50	25.04	24.00	33.02	33.15
4th	29.25	28.17	26.50	36.08	35.61
5th	30.00	31.00	29.00	39.00	38.00

TABLE 4. Quantized channel state value in the space [150 230] (arched tunnel).

	[150 158]	[158 166]	[166 174]	[174 182]	[182 190]
1st	26.43	30.61	27.68	30.67	27.67
2nd	28.04	32.49	30.16	31.91	29.56
3rd	29.65	34.33	32.57	33.16	31.39
4th	31.26	36.15	34.93	34.40	33.18
	[190 198]	[198 206]	[206 214]	[214 222]	[222 230]
1st	27.39	20.99	20.71	28.54	29.60
2nd	28.14	24.03	23.13	31.74	32.09
3rd	28.89	27.04	25.56	34.74	34.51
4th	29.64	29.86	28.00	37.66	36.89

TABLE 5. SNR thresholds in the space [150 200] (arched tunnel).

	[150 155]	[155 160]	[160 165]	[165 170]	[170 175]
1st	25.50	30.00	29.50	29.00	26.00
2nd	26.62	31.25	31.37	30.75	27.25
3rd	27.75	32.50	33.25	32.50	28.50
4th	28.87	33.75	35.12	34.25	29.75
5th	30.00	35.00	37.00	36.00	31.00
	[175 180]	[180 185]	[185 190]	[190 195]	[195 200]
1st	32.00	28.00	26.50	27.00	25.50
2nd	32.75	29.62	28.12	27.75	26.87
3rd	33.50	31.25	29.75	28.50	28.25
4th	34.25	32.87	31.37	29.25	29.62
5th	35.00	34.50	33.00	30.00	31.00

within 500 m is divided into 10 nonuniform spaces, and the lengths of these 10 spaces are 5 m, 5 m, 10 m, 15 m, 25 m, 35 m, 55 m, 80 m, 110 m and 160 m. Furthermore, each space is divided evenly into 10 sub-spaces with corresponding lengths of 0.5 m, 0.5 m, 1 m, 1.5 m, 2.5 m, 3.5 m, 5.5 m, 8 m, 11 m and 16 m. Then, the SNR threshold and the channel state quantization value in the tunnel are obtained. Consider the 8th nonuniform space as an example, as presented in Table 3 and Table 4. The state transition probability matrix of the space [174 182] is presented as (20).

Strategy 2:

First, the area that is enclosed by the SNR at the relay, X-axis and Y-axis is divided into 10 equal-area and nonoverlapping spaces, and each space is further divided into 10 sub-spaces. The FSMC channel model will be established in each sub-space, and threshold and quantitative values of the SNR can be obtained, as presented in Table 5 and Table 6. Consider the space [180 185] as an example. The state transition probability matrix is presented as (21).

$$P = \begin{pmatrix} 0.54 & 0.46 & 0 & 0 \\ 0 & 0 & 1 & 0 \\ 0 & 0 & 0 & 1 \\ 0 & 0 & 0.17 & 0.83 \end{pmatrix} \tag{20}$$

$$P = \begin{pmatrix} 1 & 0 & 0 & 0 \\ 0 & 0.5 & 0.5 & 0 \\ 0 & 0 & 0 & 1 \\ 0 & 0 & 0.33 & 0.67 \end{pmatrix} \tag{21}$$

According to the state probability transition matrix, the simulation results of the FSMC channel model in tunnel scenarios are obtained, which are presented in Figure 4.

B. NON-TUNNEL TERRAINS

In nontunnel scenarios, the two modeling methods are also used to establish FSMC wireless channel models. The SNR threshold and quantization value of each scenario are obtained via the SNR probability distribution function of
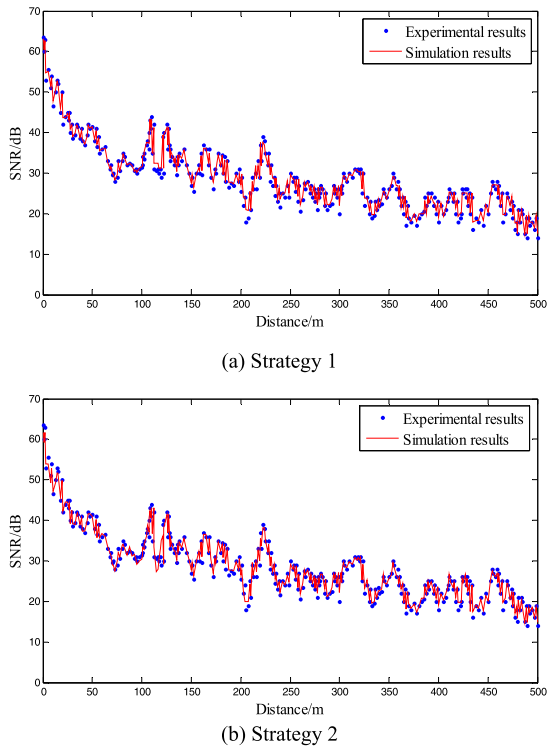
Let $D = 500$ m, let the reference distance be $d_0 = 1$ m and let the center frequency be 2.4 GHz. Then, (7) is converted to

$$\bar{\gamma}(d) = \begin{cases} 70.55 - 18.69 \log (d+1) \text{ (tunnel)} \\ 64.3 - 23.11 \log (d+1) \text{ (mountain)} \\ 119 - 42.4 \log (d+1) \text{ (viaduct)} \\ 97.5 - 36.1 \log (d+1) \text{ (cutting)} \\ 85.7 - 25.3 \log (d+1) \text{ (plain)} \end{cases} \tag{19}$$

A. TUNNEL TERRAINS

Strategy 1:

First, by using the nonuniform division method, the communication distance between the eNB and the relay

(a) Strategy 1

(b) Strategy 2

FIGURE 4. SNR quantization strategy in tunnel scenarios.

TABLE 6. Quantized channel state value in the space [150 200] (arched tunnel).

	[150 155]	[155 160]	[160 165]	[165 170]	[170 175]
1st	26.33	30.90	30.99	30.37	26.94
2nd	27.44	32.14	32.84	32.10	28.17
3rd	28.56	33.38	34.69	33.84	29.41
4th	29.67	34.62	36.55	35.57	30.65
	[175 180]	[180 185]	[185 190]	[190 195]	[195 200]
1st	32.47	29.27	27.78	27.49	26.56
2nd	33.22	30.87	29.39	28.24	27.92
3rd	33.97	32.48	31.00	28.99	29.28
4th	34.72	34.09	32.61	29.73	30.64

each scenario. Then, the state transition probability matrix of each scenario can be calculated from the threshold and the quantization value.

Consider the sub-spaces [97 105] and [135 143] as examples in the mountain scenario. The state transition probability matrices are obtained via Strategy 1 and Strategy 2 and are presented in (22) and (23), respectively.

$$P = \begin{pmatrix} 0 & 1 & 0 & 0 \\ 0.2 & 0.4 & 0.4 & 0 \\ 0 & 0.5 & 0 & 0.5 \\ 0 & 0 & 0 & 1 \end{pmatrix} \quad \text{(Strategy 1)} \quad (22)$$

$$P = \begin{pmatrix} 0.5 & 0.5 & 0 & 0 \\ 0 & 0 & 1 & 0 \\ 0.25 & 0.5 & 0.25 & 0 \\ 0 & 0 & 0 & 1 \end{pmatrix} \quad \text{(Strategy 2)} \quad (23)$$

Consider the sub-spaces [50 60] and [130 138] as examples in the viaduct scenario. The state transition probability matrices are obtained via Strategy 1 and Strategy 2 and are presented in (24) and (25), respectively.

$$P = \begin{pmatrix} 1 & 0 & 0 & 0 \\ 0.25 & 0.75 & 0 & 0 \\ 0 & 1 & 0 & 0 \\ 0 & 0 & 0.5 & 0.5 \end{pmatrix} \quad \text{(Strategy 1)} \quad (24)$$

$$P = \begin{pmatrix} 0 & 1 & 0 & 0 \\ 0.5 & 0.5 & 0 & 0 \\ 0 & 1 & 0 & 0 \\ 0 & 0 & 0.5 & 0.5 \end{pmatrix} \quad \text{(Strategy 2)} \quad (25)$$

Consider the sub-spaces [40 48] and [126 135] as examples in the cutting scenario. The state transition probability matrices are obtained via Strategy 1 and Strategy 2 and presented in (26) and (27), respectively.

$$P = \begin{pmatrix} 0 & 1 & 0 & 0 \\ 0.33 & 0.34 & 0.33 & 0 \\ 0 & 1 & 0 & 0 \\ 0 & 0 & 1 & 0 \end{pmatrix} \quad \text{(Strategy 1)} \quad (26)$$

$$P = \begin{pmatrix} 0 & 1 & 0 & 0 \\ 0.5 & 0.5 & 0 & 0 \\ 0 & 0 & 0.33 & 0.67 \\ 0 & 0 & 0.5 & 0.5 \end{pmatrix} \quad \text{(Strategy 2)} \quad (27)$$

Consider the sub-spaces [131 145] and [126 133] as examples in the plain scenario. The state transition probability matrices are obtained via Strategy 1 and Strategy 2 and are presented in (28) and (29), respectively.

$$P = \begin{pmatrix} 0.66 & 0.34 & 0 & 0 \\ 0 & 1 & 0 & 0 \\ 0 & 0 & 0.71 & 0.29 \\ 0 & 0 & 0.5 & 0.5 \end{pmatrix} \quad \text{(Strategy 1)} \quad (28)$$

$$P = \begin{pmatrix} 0 & 1 & 0 & 0 \\ 0.33 & 0 & 0.67 & 0 \\ 0 & 0.5 & 0 & 0.5 \\ 0 & 0 & 0 & 1 \end{pmatrix} \quad \text{(Strategy 2)} \quad (29)$$

It is worth noting that the time that the state transition matrix remains unchanged is related to the speed of the trains. In this paper, the distance of 500 m between the eNB and the train is firstly divided into 10 nonuniform spaces, and then each space is equally divided into 10 sub-spaces, and the state transition matrix is established in each sub-space. Taking the mountain scenario as an example, for the average speed of the high-speed train in the mountain is 200 km/h, the longest time for the state transition matrix to remain unchanged is about 3.6s, and the shortest time is about 0.18s.

Figure (5) - Figure (8) present the simulation results of the FSMC channel models in the mountain, viaduct, cutting
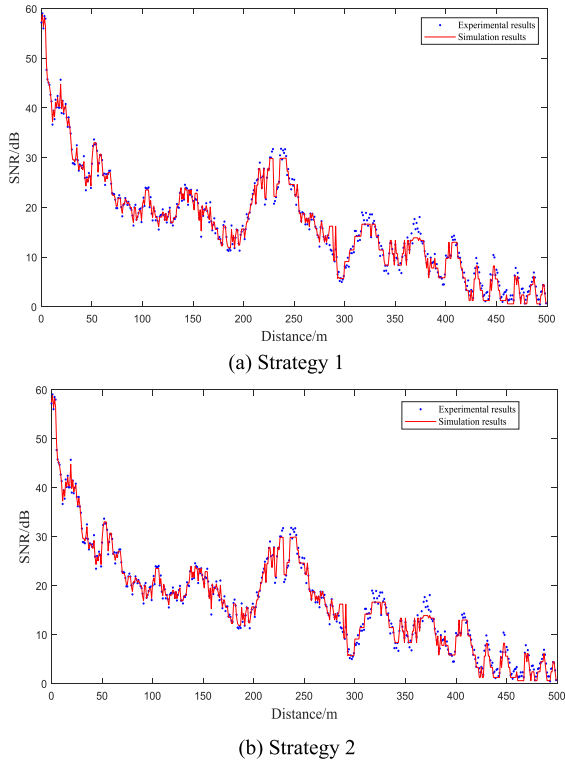
(a) Strategy 1

(b) Strategy 2

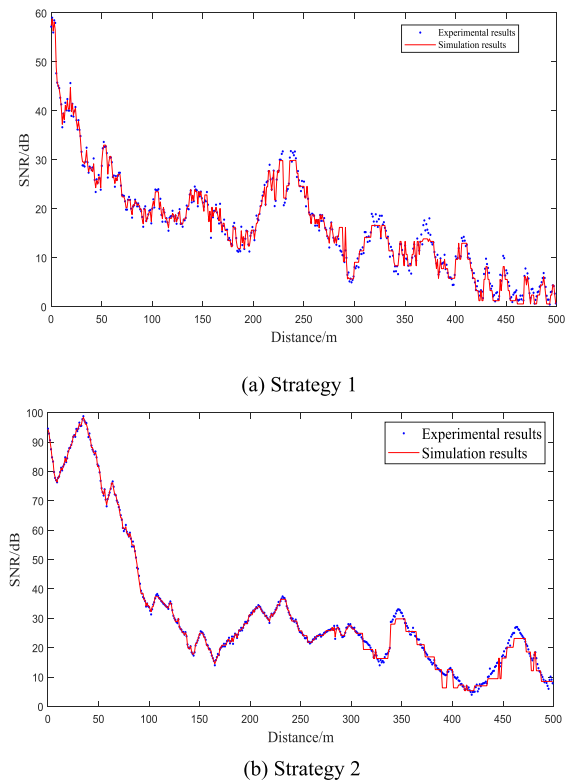**FIGURE 5.** SNR in mountain scenarios.

(a) Strategy 1

(b) Strategy 2

FIGURE 6. SNR in viaduct scenarios.

and plain scenarios, respectively, that were constructed via Strategy 1 and the Strategy 2.
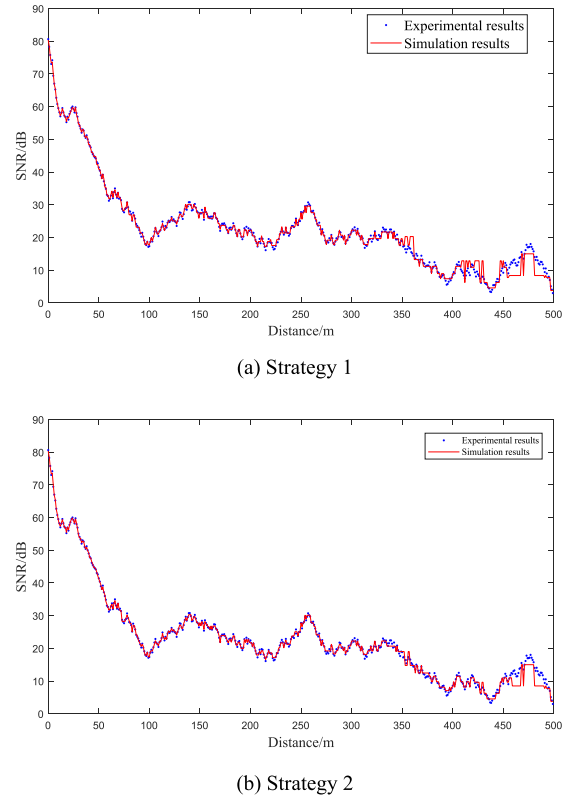

(a) Strategy 1

(b) Strategy 2

FIGURE 7. SNR in cutting scenarios.

TABLE 7. MSE for FSMC channel model.

	tunnels	mountains	viaducts	cuttings	plains
MSE1	0.55	2.55	2.11	2.07	1.003
MSE2	0.81	1.2	1.87	1.08	1.01
MSE3	1.79	4.39	3.32	2.47	1.21

To describe more intuitively the accuracies of the FSMC models in various HSR scenarios, the MSE indicator is used. Let MSE1, MSE2 and MSE3 represents the MSE values of FSMC channel model based on nonuniform space division SNR quantization strategy, equal-area space division SNR quantization strategy and uniform space division SNR quantization strategy [19], respectively. By calculating the MSE of the source data and the simulation results of the FSMC model, the MSE values for the FSMC channel models are obtained, in Table 7. The accuracy of the model constructed by using the two nonuniform space division strategies and the uniform space division strategy is analyzed and compared.

According to Table 7, when the train is in a tunnel scenario, the accuracy of the FSMC model that is derived via Strategy 1 is higher than that of the model that is derived via Strategy 2; when the train is in the plain scenario, the MSEs of the FSMC models that are obtained via the two modeling strategies are approximately equal; when the train is in other HSR scenarios, the FSMC model based on Strategy 2 has the higher accuracy. The MSE of uniform space division strategy is higher than that of Strategy 1 and Strategy 2.
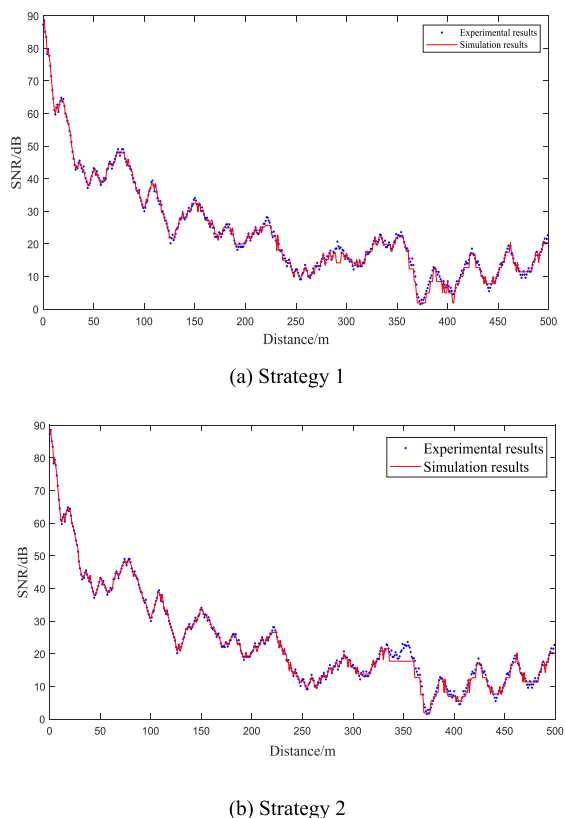
(a) Strategy 1

(b) Strategy 2

FIGURE 8. SNR in plain scenarios.

It shows that the nonuniform space division strategy performs well compared with the uniform interval division strategy in the FSMC wireless channel modeling for the HSR scenarios.

VI. CONCLUSIONS

In this paper, the problems of poor universality and low modeling accuracy of HSR wireless channel models are studied. The nonuniform space division SNR quantization strategy and the equal-area space division SNR quantization strategy are adopted. The mathematical relationships among the SNR threshold, channel state and state probability transition matrix are analyzed, and a novel FSMC simulation model for various HSR scenarios is established. The simulation results that were obtained using the proposed FSMC model closely fit the experimental results; therefore, the proposed simulation model can better track the channel state in various HSR scenarios and realizes higher modeling accuracy.

In this paper, the influence of shadow fading on the fading of the SNR is not considered in the FSMC path-loss modeling experiments for various HSR scenarios, which will be further studied. In addition, the effect of space division interval and the number of Markov state on the accuracy of FSMC model will be investigated in the future work.

REFERENCES

[1] T. Zhou, H. Li, Y. Wang, L. Liu, and C. Tao, "Channel modeling for future high-speed railway communication systems: A survey," *IEEE Access*, vol. 7, pp. 52818–52826, 2019, doi: 10.1109/ACCESS.2019.2912408.

[2] J. Yang, B. Ai, S. Salous, K. Guan, D. He, G. Shi, and Z. Zhong, "An efficient MIMO channel model for LTE-R network in high-speed train environment," *IEEE Trans. Veh. Technol.*, vol. 68, no. 4, pp. 3189–3200, Apr. 2019, doi: 10.1109/TVT.2019.2894186.

[3] X. Wang, G. Wang, R. Fan, and B. Ai, "Channel estimation with expectation maximization and historical information based basis expansion model for wireless communication systems on high speed railways," *IEEE Access*, vol. 6, pp. 72–80, 2018, doi: 10.1109/ACCESS.2017.2745708.

[4] B. Ai, C. Briso-Rodriguez, X. Cheng, T. Kurner, Z.-D. Zhong, K. Guan, R.-S. He, L. Xiong, D. W. Matolak, and D. G. Michelson, "Challenges toward wireless communications for high-speed railway," *IEEE Trans. Intell. Transp. Syst.*, vol. 15, no. 5, pp. 2143–2158, Oct. 2014, doi: 10.1109/TITS.2014.2310771.

[5] Y. Zhou and B. Ai, "Handover schemes and algorithms of high-speed mobile environment: A survey," *Comput. Commun.*, vol. 47, no. 1, pp. 1–15, Jul. 2014, doi: 10.1016/j.comcom.2014.04.005.

[6] J. Bok and H.-G. Ryu, "Path loss model considering Doppler shift for high speed railroad communication," in *Proc. 16th Int. Conf. Adv. Commun. Technol.*, Pyeongchang, South Korea, Feb. 2014, pp. 1–4.

[7] S. Wei, B. Ai, D. He, K. Guan, L. Wang, and Z. Zhong, "Calibration of ray-tracing simulator for millimeter-wave outdoor communications," in *Proc. IEEE Int. Symp. Antennas Propag. USNC/URSI Nat. Radio Sci. Meeting*, San Diego, CA, USA, Jul. 2017, pp. 1907–1908.

[8] L. Wang, K. Guan, B. Ai, G. Li, D. He, R. He, L. Tian, J. Dou, and Z. Zhong, "An accelerated algorithm for ray tracing simulation based on high-performance computation," in *Proc. 11th Int. Symp. Antennas, Propag. EM Theory (ISAPE)*, Guilin, China, Oct. 2016, pp. 512–515.

[9] L. Ma, K. Guan, D. He, G. Li, S. Lin, B. Ai, and Z. Zhong, "Ray-tracing simulation and analysis for air-to-ground channel in railway environment," in *Proc. IEEE Int. Symp. Antennas Propag. USNC/URSI Nat. Radio Sci. Meeting*, Boston, MA, USA, Jul. 2018, pp. 1–2.

[10] J. Yang, B. Ai, K. Guan, D. He, X. Lin, B. Hui, J. Kim, and A. Hrovat, "A geometry-based stochastic channel model for the millimeter-wave band in a 3GPP high-speed train scenario," *IEEE Trans. Veh. Technol.*, vol. 67, no. 5, pp. 3853–3865, May 2018.

[11] B. Chen, Z. Zhong, and B. Ai, "Stationarity intervals of time-variant channel in high speed railway scenario," *China Commun.*, vol. 9, no. 8, pp. 64–70, Aug. 2012.

[12] T. Zhou, C. Tao, S. Salous, and L. Liu, "Measurements and analysis of angular characteristics and spatial correlation for high-speed railway channels," *IEEE Trans. Intell. Transp. Syst.*, vol. 19, no. 2, pp. 357–367, Feb. 2018, doi: 10.1109/TITS.2017.2681112.

[13] Y. Zhang, Z. He, W. Zhang, L. Xiao, and S. Zhou, "Measurement-based delay and Doppler characterizations for high-speed railway hilly scenario," *Int. J. Antennas Propag.*, vol. 2014, no. 4, pp. 1–8, 2014, doi: 10.1155/2014/875345.

[14] L. Liu, C. Tao, R. Sun, H. Chen, and Z. Lin, "Markov chain based channel characterization for high speed railway in viaduct scenarios," in *Proc. IEEE Int. Conf. Commun. (ICC)*, Sydney, NSW, Australia, Jun. 2014, pp. 5896–5901.

[15] R. Zhang and L. Cai, "Markov modeling for data block transmission of OFDM systems over fading channels," in *Proc. IEEE Int. Conf. Commun.*, Dresden, Germany, Jun. 2009, pp. 14–18.

[16] S. Lin, Y. L. Li, Y. Li, B. Ai, and Z. Zhong, "Finite-state Markov channel modeling for vehicle-to-infrastructure communications," in *Proc. IEEE 6th Int. Symp. Wireless Veh. Commun. (WiVeC)*, Vancouver, BC, Canada, Sep. 2014, pp. 1–5.

[17] A. Abdul Salam, R. Sheriff, S. Al-Araji, K. Mezher, and Q. Nasir, "Novel approach for modeling wireless fading channels using a finite state Markov Chain," *ETRI J.*, vol. 39, no. 5, pp. 718–728, Oct. 2017, doi: 10.4218/etrij.17.0117.0246.

[18] S. Lin, Z. Zhong, L. Cai, and Y. Luo, "Finite state Markov modelling for high speed railway wireless communication channel," in *Proc. IEEE Global Commun. Conf. (GLOBECOM)*, Anaheim, CA, USA, Dec. 2012, pp. 5421–5426.

[19] X. Lv, J. Li, X. Jia, and B. Yang, "Modeling for train-ground communication channel based on WSN," in *Proc. 27th Chin. Control Decis. Conf. (CCDC)*, Qingdao, China, May 2015, pp. 5241–5245.

[20] H. Wang, F. R. Yu, L. Zhu, T. Tang, and B. Ning, "Finite-state Markov modeling for wireless channels in tunnel communication-based train control systems," *IEEE Trans. Intell. Transp. Syst.*, vol. 15, no. 3, pp. 1083–1090, Jun. 2014, doi: 10.1109/tits.2014.2298038.

[21] R. He, Z. Zhong, B. Ai, G. Wang, J. Ding, and A. F. Molisch, "Measurements and analysis of propagation channels in high-speed railway viaducts," *IEEE Trans. Wireless Commun.*, vol. 12, no. 2, pp. 794–805, Feb. 2013, doi: 10.1109/TWC.2012.120412.120268.

[22] C. Zhang, G. Wang, M. Jia, R. He, L. Zhou, and B. Ai, "Doppler shift estimation for millimeter-wave communication systems on high-speed railways," *IEEE Access*, vol. 7, pp. 40454–40462, 2019, doi: 10.1109/ACCESS.2018.2861889.

[23] K. Guan, B. Ai, Z. Zhong, C. F. Lopez, L. Zhang, C. Briso-Rodriguez, A. Hrovat, B. Zhang, R. He, and T. Tang, "Measurements and analysis of large-scale fading characteristics in curved subway tunnels at 920 MHz, 2400 MHz, and 5705 MHz," *IEEE Trans. Intell. Transp. Syst.*, vol. 16, no. 5, pp. 2393–2405, Oct. 2015, doi: 10.1109/TITS.2015.2404851.

[24] Y. Zhang, Y. Liu, J. Sun, C.-X. Wang, and X. Ge, "Impact of different parameters on channel characteristics in a high-speed train ray tracing tunnel channel model," in *Proc. IEEE 85th Veh. Technol. Conf. (VTC Spring)*, Sydney, NSW, Australia, Jun. 2017, pp. 1–5.

[25] S. Lin, L. Kong, L. He, K. Guan, B. Ai, Z. Zhong, and C. Briso-Rodriguez, "Finite-state Markov modeling for high-speed railway fading channels," *IEEE Antennas Wireless Propag. Lett.*, vol. 14, pp. 954–957, 2015, doi: 10.1109/lawp.2015.2388701.

[26] X. Li, C. Shen, A. Bo, and G. Zhu, "Finite-state Markov modeling of fading channels: A field measurement in high-speed railways," in *Proc. IEEE/CIC Int. Conf. Commun. China (ICCC)*, Xi'an, China, Aug. 2013, pp. 577–582.

[27] B. Zhang, Z. Zhong, R. He, F. Tufvesson, and B. Ai, "Measurement-based multiple-scattering model of small-scale fading in high-speed railway cutting scenarios," *IEEE Antennas Wireless Propag. Lett.*, vol. 16, pp. 1427–1430, 2016, doi: 10.1109/LAWP.2016.2626303.

[28] R. He, Z. Zhong, B. Ai, J. Ding, and Y. Yang, "Propagation measurements and analysis of fading behavior for high speed rail cutting scenarios," in *Proc. IEEE Global Commun. Conf. (GLOBECOM)*, Anaheim, CA, USA, Dec. 2012, pp. 5015–5020.

[29] H. Popovic, D. Stefanovic, A. Mitic, I. Stefanovic, and D. Stefanovic, "Some statistical characteristics of Nakagami-*m* distribution," in *Proc. 8th Int. Conf. Telecommun. Modern Satell., Cable Broadcast. Services*, Nis, Serbia, Sep. 2007, pp. 509–512.

[30] G. Kai, "FSMC model for Nakagami-*m* distribution fading channels and its performance analysis," *Signal Process.*, vol. 22, no. 2, pp. 275–277, 2006.

[31] C. Iskander and P. T. Mathiopoulos, "Fast simulation of diversity Nakagami fading channels using finite-state Markov models," *IEEE Trans. Broadcast.*, vol. 49, no. 3, pp. 269–277, Sep. 2003, doi: 10.1109/tbc.2003.817096.

[32] W. Cao, X. Li, W. Hu, J. Lei, and W. Zhang, "OFDM reference signal reconstruction exploiting subcarrier-grouping-based multi-level Lloyd-Max algorithm in passive radar systems," *IET Radar, Sonar Navigat.*, vol. 11, no. 5, pp. 873–879, May 2017, doi: 10.1049/iet-rsn.2016.0340.

JIANLI XIE was born in Gansu, China, in 1972. He received the B.Sc. degree from Sichuan University, in 1993, and the master's and Ph.D. degrees from the School of Electronics and Information Engineering, Lanzhou Jiaotong University, in 1999 and 2014, respectively. From 1993 to 1996, he worked as an Engineer with Lanzhou General Machinery Plant. From 1999 to 2007, he was a Senior Hardware Engineer with Beijing Great Dragon Company. He is currently working as a Professor with Lanzhou Jiaotong University. He has published over 20 scientific articles in his research area till now. His research interests include railway wireless communication and cognitive radio techniques.

CUIRAN LI (Member, IEEE) was born in Shanxi, China, in 1975. She received the bachelor's and master's degrees from the Department of Communication Engineering, Lanzhou Jiaotong University, in 1996 and 1999, respectively, and the Ph.D. degree from the School of Electronics and Information Engineering, Beijing Jiaotong University, in 2003. She is currently working as a Professor with Lanzhou Jiaotong University. She has published a book and over 40 scientific articles in her research area till now. Her research interests include railway mobile communication, wireless sensor networks, and cooperative communication technology.

WENBO ZHANG is currently pursuing the master's degree with the School of Electronic and Information Engineering, Lanzhou Jiaotong University. His research interest includes wireless channel modeling and simulation in high-speed rail mountain environment.

LING LIU is currently pursuing the master's degree with the School of Electronic and Information Engineering, Lanzhou Jiaotong University. Her research interest includes wireless channel modeling and optimization in HSR environments.

• • •